

COMPUTATION OF DYNAMIC STRESS INTENSITY FACTORS IN FGMS BY AN ADVANCED LBIEM

Jan Sladek¹, Vladimir Sladek¹ and Ch. Zhang²

¹Institute of Construction and Architecture, Slovak Academy of Sciences, 84503 Bratislava, Slovakia

²Department of Civil Engineering, University of Applied Sciences Zittau/Görlitz, D-02763 Zittau, Germany

ABSTRACT

An advanced meshless local boundary integral equation method (LBIEM) is presented for computing dynamic stress intensity factors in continuously nonhomogeneous functionally graded materials (FGMs). Interior nodes are introduced which are randomly spread in the analyzed domain and each one is surrounded by a circular subdomain centered at the collocation point. Elastostatic fundamental solutions for homogeneous materials are applied, which results in a boundary-domain integral formulation. By using modified elastostatic fundamental solutions vanishing on the boundary of the subdomain, the unknown traction vector can be eliminated from the local boundary integral equations (BIEs) for all interior nodes. The spatial variation of the displacements is approximated by the moving least squares (MLS) scheme. Laplace-transform technique is used to solve the arising initial-boundary problems.

1 INTRODUCTION

Functionally graded materials (FGMs) represent a new class of composites designed to achieve high performance levels superior to that of homogeneous materials by combining the desirable properties of each constituent. FGMs have no interfaces or interphases and are hence advantageous over conventional composites and laminates. They can be applied to a wide range of engineering structures and components such as electronic devices, corrosion-resistant and wear-resistant coatings, thermal barrier coatings and biomaterials. The fracture and damage behavior of FGMs is essential to their integrity, reliability and durability in engineering applications. However, most of previous investigations on fracture analysis of FGMs have been devoted to static or quasi-static loading conditions, and only few studies on transient dynamic fracture analysis of FGMs have been reported in literature due to the complexity of the arising initial-boundary value problems.

For FGMs with continuously nonhomogeneous material properties, the initial-boundary value problem of transient dynamic crack analysis is governed by partial differential equations with variable coefficients. In principle, both the domain-type methods (such as the finite element method, the finite difference method, and the finite volume method) and the boundary-type methods (such as the boundary integral equation method and the boundary element method) can be applied to transient dynamic crack analysis in FGMs. The boundary integral equation method (BIEM) or the boundary element method (BEM) is especially attractive due to the possible dimension reduction of a boundary value problem governed by linear partial differential equations. However, a pure boundary integral formulation is possible only if the fundamental solutions or the Green's functions of the original partial differential equations are available in analytical or simple forms. For homogeneous materials, both time-domain and Laplace-transformed dynamic fundamental solutions are available. In contrast, for general FGMs, neither time-domain nor Laplace-transformed dynamic fundamental solutions can be given in closed and simple forms, which prohibits a successful numerical implementation of the BIEs. To overcome this difficulty, one can introduce a parametric or Levi function instead of the fundamental solutions. A parametric correctly describes the main part of the fundamental solutions but it is not required to exactly satisfy the original differential equations. In this paper, an advanced meshless local boundary integral equation method (LBIEM) is presented for computing dynamic stress intensity factors in

FGMs. In our method, the elastostatic fundamental solutions for homogeneous materials is used, which results in a boundary-domain integral formulation. Local boundary integral equations (LBIEs) are then applied to small subdomains, which cover the analyzed domain of the FGMs. On the artificial boundary of the subdomains lying in the interior of the body, both the displacement and the traction vectors are unknown. To eliminate the number of unknowns, either the fundamental solution or the corresponding traction vector should vanish on the boundary of the subdomains. For this purpose, the method based on the companion solutions is adopted in our analysis. Laplace-transform technique is used to convert the hyperbolic elastodynamic governing equations into the elliptical partial differential equations. After solving several quasi-static boundary value problems for discrete values of the Laplace-transform parameter, the Stehfest's inversion method is then used to obtain the time-dependent solutions. The spatial variation of the displacements is approximated by the moving least-squares (MLS) scheme. The efficiency and the accuracy of the advanced meshless LBIEM are verified by numerical examples for dynamic crack analysis in FGMs.

2 PROBLEM STATEMENT AND LOCAL BOUNDARY INTEGRAL EQUATIONS

Let us consider an isotropic, non-homogeneous and linear elastic solid with Young's modulus $E(\mathbf{x})$ being dependent on Cartesian coordinates and the Poisson's ratio ν being constant. In this case, the elasticity tensor can be written as

$$c_{ijkl}(\mathbf{x}) = \mu(\mathbf{x})c_{ijkl}^0, \quad (1)$$

$$\mu(\mathbf{x}) = \frac{E(\mathbf{x})}{2(1+\nu)}, \quad c_{ijkl}^0 = 2\nu/(1-2\nu)\delta_{ij}\delta_{kl} + \delta_{ik}\delta_{jl} + \delta_{il}\delta_{jk}. \quad (2)$$

In eqns (1) and (2), $\mu(\mathbf{x})$ represents the shear modulus, and δ_{ij} denotes the Kronecker delta. In terms of displacements, the equations of motion for a non-homogeneous solid can be written as

$$\mu u_{i,kk} + \frac{\mu}{1-2\nu} u_{k,ki} = -X_i - \mu_{,i} \frac{2\nu}{1-2\nu} u_{k,k} - \mu_{,j} (u_{i,j} + u_{j,i}) + \rho \ddot{u}_i, \quad (3)$$

where u_i and X_i are the components of the time-dependent displacement and body force vectors, ρ is the mass density of the material, a comma after a quantity represents spatial derivatives, while superscript dots indicate partial derivatives with respect to time, respectively.

Application of the Laplace-transform to the equations of motion (3) yields

$$\mu \bar{u}_{i,kk} + \frac{\mu}{1-2\nu} \bar{u}_{k,ki} + \bar{F}_i + \bar{g}_i - \rho p^2 \bar{u}_i = 0, \quad (4)$$

where $\bar{g}_i(\mathbf{x}, p) = \mu_{,i}(\mathbf{x}) \frac{2\nu}{1-2\nu} \bar{u}_{k,k}(\mathbf{x}, p) + \mu_{,j}(\mathbf{x}) [\bar{u}_{i,j}(\mathbf{x}, p) + \bar{u}_{j,i}(\mathbf{x}, p)]$, and

$$\bar{F}_i(\mathbf{x}, p) = \bar{X}_i(\mathbf{x}, p) + p u_i(\mathbf{x}) + \dot{u}_i(\mathbf{x})$$

is a redefined body force vector in the Laplace-transformed domain with the initial boundary conditions for the displacements $u_i(\mathbf{x})$ and the velocities $\dot{u}_i(\mathbf{x})$, and p is the Laplace-transform parameter.

By using elastostatic fundamental solutions for homogeneous materials, we obtain the following integral representation for the displacements [1]

$$\begin{aligned} \bar{u}_j(\mathbf{y}, p) = & \int_{\Gamma} \frac{1}{\mu(\mathbf{x})} \bar{t}_i(\mathbf{x}, p) U_{ij}(\mathbf{x}, \mathbf{y}) d\Gamma - \int_{\Gamma} T_{ij}(\mathbf{x}, \mathbf{y}) \bar{u}_i(\mathbf{x}, p) d\Gamma + \\ & + \int_{\Omega} \frac{1}{\mu(\mathbf{x})} [\bar{F}_i(\mathbf{x}, p) + \bar{g}_i(\mathbf{x}, p) - \rho p^2 \bar{u}_i(\mathbf{x}, p)] U_{ij}(\mathbf{x}, \mathbf{y}) d\Omega, \quad \text{for } \mathbf{y} \notin \Gamma, \end{aligned} \quad (5)$$

where $U_{ij}(\mathbf{x}, \mathbf{y})$ and $T_{ij}(\mathbf{x}, \mathbf{y})$ represent the elastostatic displacement and traction fundamental solutions for a homogeneous material with $\mu = 1$, and

$$\bar{t}_i(\mathbf{x}, p) = \mu(\mathbf{x}) \left\{ \frac{2\nu}{1-2\nu} \bar{u}_{k,k}(\mathbf{x}, p) n_i + [\bar{u}_{i,k}(\mathbf{x}, p) + \bar{u}_{k,i}(\mathbf{x}, p)] n_k \right\} \quad (6)$$

is the traction vector with the unit outward normal vector n_i to the boundary Γ .

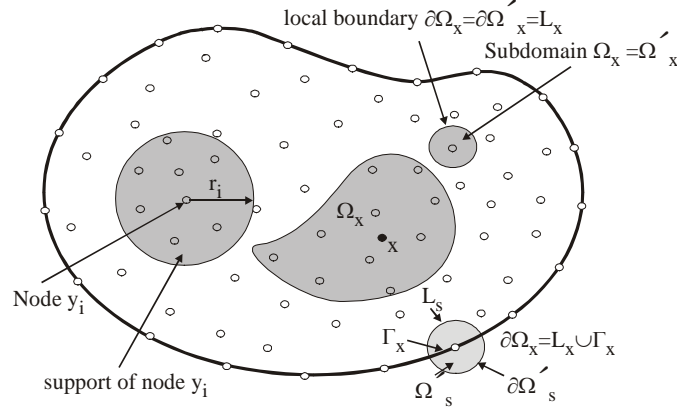


Fig. 1: Local boundaries, support of nodes and domain of definition of the MLS approximation

If, instead of the entire domain Ω of the given problem, we consider a sub-domain Ω_s (see Fig. 1), which is located entirely inside Ω , we obtain the following integral representation for the displacements in the interior of Ω_s

$$\begin{aligned} \bar{u}_j(\mathbf{y}, p) = & \int_{\partial\Omega_s} \frac{1}{\mu(\mathbf{x})} \bar{t}_i(\mathbf{x}, p) U_{ij}(\mathbf{x}, \mathbf{y}) d\Gamma - \int_{\partial\Omega_s} T_{ij}(\mathbf{x}, \mathbf{y}) \bar{u}_i(\mathbf{x}, p) d\Gamma + \\ & + \int_{\Omega_s} \frac{1}{\mu(\mathbf{x})} [\bar{F}_i(\mathbf{x}, p) + \bar{g}_i(\mathbf{x}, p) - \rho p^2 \bar{u}_i(\mathbf{x}, p)] U_{ij}(\mathbf{x}, \mathbf{y}) d\Omega, \end{aligned} \quad (7)$$

where $\partial\Omega_s$ is the boundary of the sub-domain Ω_s . Collocating the integral representation (7) at interior nodes $\mathbf{y}_s \in \Omega_s$ in a meshless approach with an approximation of the displacement field, LBIEs for computing the unknown nodal values are obtained.

On the artificial boundary $\partial\Omega_s$, both the displacement and the traction vectors are unknown. If the fundamental solutions $U_{ij}(\mathbf{x}, \mathbf{y})$ were vanishing on the boundary of the sub-domain $\partial\Omega_s$, the integral containing the traction vector could be eliminated. This can be achieved by using a companion solution [2]. The companion solution \tilde{U}_{ij} is associated with the elastostatic displacement fundamental solutions U_{ij} and is the solution to the following equations

$$c_{imkl} \tilde{U}_{kj,lm} = 0 \quad \text{on } \Omega'_s, \quad \tilde{U}_{ij} = U_{ij} \quad \text{on } \partial\Omega'_s, \quad (8)$$

with Ω'_s being a circle of the radius r_0 , which coincides with Ω_s for interior nodes (see Fig. 1).

The modified displacement fundamental solutions $U_{ij}^* = U_{ij} - \tilde{U}_{ij}$ have to satisfy the same

governing equations as for U_{ij} . On the boundary of the circular domain $\partial\Omega'_s$, these fundamental solutions are identically zero due to the second condition in (8). Hence, eqn (7) can be rewritten as

$$\bar{u}_j(\mathbf{y}, p) = - \int_{\partial\Omega_s} T_{ij}^*(\mathbf{x}, \mathbf{y}) \bar{u}_i(\mathbf{x}, p) d\Gamma + \int_{\Omega_s} \frac{1}{\mu(\mathbf{x})} [\bar{F}_i(\mathbf{x}, p) + \bar{g}_i(\mathbf{x}, p) - \rho p^2 \bar{u}_i(\mathbf{x}, p)] U_{ij}^*(\mathbf{x}, \mathbf{y}) d\Omega \quad (9)$$

for the source point \mathbf{y} located inside $\Omega_s \subset \Omega$. Explicit expressions for the modified elastostatic fundamental solutions U_{ij}^* and T_{ij}^* can be found in [3]. If a source point is located on the global boundary $\zeta_s \in \Gamma_s \subset \Gamma$, the LBIEs can be written as

$$\begin{aligned} \bar{u}_j(\zeta_s, p) + \int_{L_s} T_{ij}^*(\mathbf{x}, \zeta_s) \bar{u}_i(\mathbf{x}, p) d\Gamma + \lim_{\mathbf{y} \rightarrow \zeta_s} \int_{\Gamma_s} T_{ij}^*(\mathbf{x}, \mathbf{y}) \bar{u}_j(\mathbf{x}, p) d\Gamma - \int_{\Gamma_s} \frac{1}{\mu(\mathbf{x})} \bar{t}_i(\mathbf{x}, p) U_{ij}^*(\mathbf{x}, \zeta_s) d\Gamma = \\ = \int_{\Omega_s} \frac{1}{\mu(\mathbf{x})} [\bar{F}_i(\mathbf{x}, p) + \bar{g}_i(\mathbf{x}, p) - \rho p^2 \bar{u}_i(\mathbf{x}, p)] U_{ij}^*(\mathbf{x}, \zeta_s) d\Omega \quad . \end{aligned} \quad (10)$$

3 A MESHLESS METHOD FOR LOCAL BOUNDARY INTEGRAL EQUATIONS

A numerical solution procedure for solving the LBIEs (9) and (10) is developed. The method is a meshless method, which is based on the moving least squares (MLS) approximation. According to the MLS scheme, the function to be approximated can be written as [4]

$$\bar{\mathbf{u}}(\mathbf{x}, p) = \mathbf{\Phi}^T(\mathbf{x}) \hat{\mathbf{u}} = \sum_{j=1}^n \phi_j(\mathbf{x}) \hat{\mathbf{u}}_j(p) \quad , \quad (11)$$

in which $\phi_j(\mathbf{x})$ denotes the shape functions associated with node j , and $\hat{\mathbf{u}}_j(p)$ are fictitious parameters. Substitution of the MLS approximation (11) into eqn (6) yields the following approximation formula for the traction vector

$$\bar{\mathbf{t}}(\mathbf{x}, p) = \mathbf{N}(\mathbf{x}) \mathbf{D} \sum_{j=1}^n B_j(\mathbf{x}) \hat{\mathbf{u}}_j(p) \quad , \quad (12)$$

where the matrix $\mathbf{N}(\mathbf{x})$ corresponds to the normal vector at \mathbf{x} , \mathbf{D} is the stress-strain matrix and the matrix $B_j(\mathbf{x})$ represents the gradients of the shape functions at \mathbf{x} .

Substitution of the MLS approximations (11) and (12) into the LBIEs (9) and (10) leads to a system of linear algebraic equations for $\hat{\mathbf{u}}_j(p)$. Then, the displacement and the stress components at any point can be computed numerically for discrete values of the Laplace-transform parameter. Subsequently, the corresponding time-dependent solutions can be obtained by an inverse Laplace-transform. In the present analysis, the sophisticated Stehfest's algorithm [5] is applied.

4 NUMERICAL EXAMPLES AND DISCUSSIONS

As numerical examples, we consider a rectangular plate with an edge crack as depicted in Fig. 2. The plate has the length $2h = 30$, width $b = 10$, and crack length $a = 0.4b$. At the top and the bottom sides of the plate, a uniform impact tensile stress $\sigma_{22}(t) = \sigma H(t)$ is applied. The elastic modulus is assumed to have an exponential graduation described by

$$E(x_1) = E_1 \exp(\gamma x_1) \quad , \quad 0 \leq x_1 \leq b \quad , \quad (31)$$

where $E_1 = E(0)$, $E_2 = E(b)$ and $\gamma = b^{-1} \ln(E_2/E_1)$. Poisson's ratio is taken as $\nu = 0.25$ and $E_1 = 10^4 \text{ N/mm}^2$.

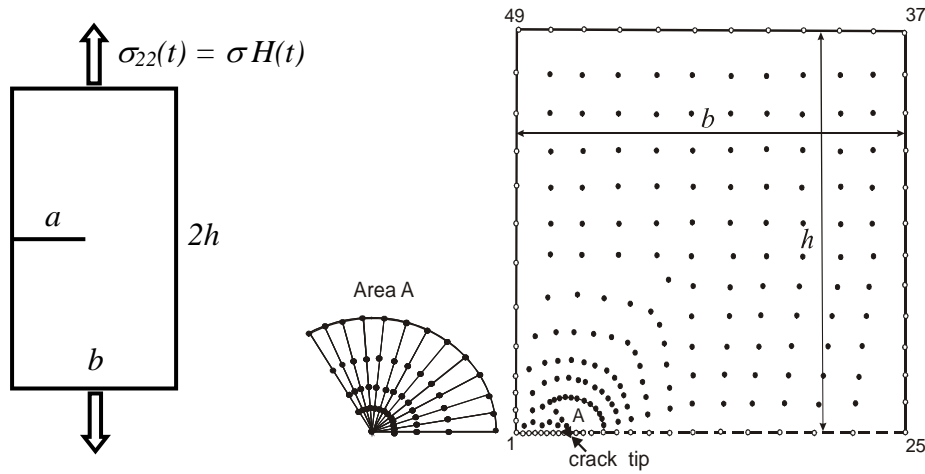


Fig. 2: Node distribution in an half of a rectangular plate with an edge crack

Due to symmetry of the geometry and the loading, only one half of the plate as shown in Fig. 2 is analyzed by the LBIEM. In this case, only the mode I dynamic stress intensity factor occurs. The LBIEM model consists of total 230 nodes which include 61 boundary nodes. The node density is progressively increasing towards the crack-tip. For convenience, the dynamic stress intensity factor is normalized by its corresponding static value $K_I^{stat} = \sigma\sqrt{\pi a}$.

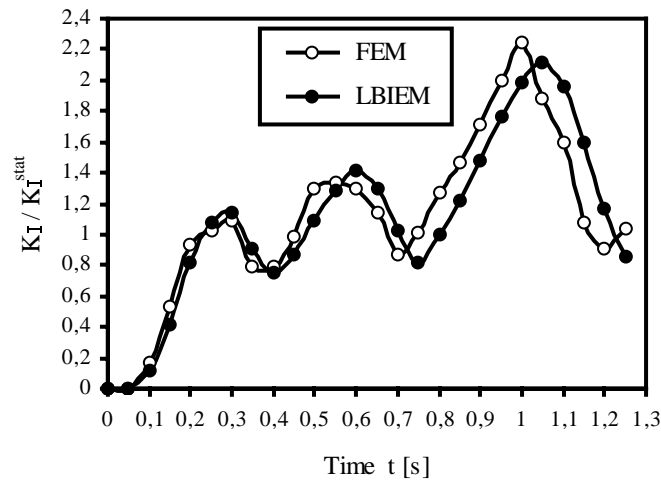


Fig. 3: Normalized dynamic stress intensity factor for a FGM plate with $E_2 / E_1 = 5$

To test the accuracy of the present meshless LBIEM, a static loading is first considered. The normalized stress intensity factors for different ratios of E_2 / E_1 are compared with those by Kim and Paulino [6] and our FEM analysis by using a very fine mesh with 5472 quadrilateral 8-node elements and 16723 nodes in the commercial NASTRAN code. Our numerical results agree very well with those obtained by FEM. Another check has been made for a cracked homogeneous plate under an impact tension. The same node number and distribution as in the static loading case have

been used. The Stehfest's method for the Laplace inversion is applied. Numerical results are compared with those provided by the NASTRAN code, which show again a quite good agreement. For a cracked FGM plate under an impact tensile loading, numerical calculations have been carried out for a constant mass density $\rho = 1 \text{ kg/cm}^2$ and two different ratios $E_2/E_1 = 5$ and 0.2 . The corresponding normalized dynamic stress intensity factors are presented in Figs. 3 and 4 versus time. The first peak of the mode I stress intensity factors increases with increasing gradient parameter γ . A comparison of our numerical results with that obtained by the FEM-NASTRAN code shows a fairly good agreement.

In conclusion, the meshless LBIEM presented in this paper provides an accurate and efficient numerical tool for computing transient dynamic stress intensity factors in FGMs.

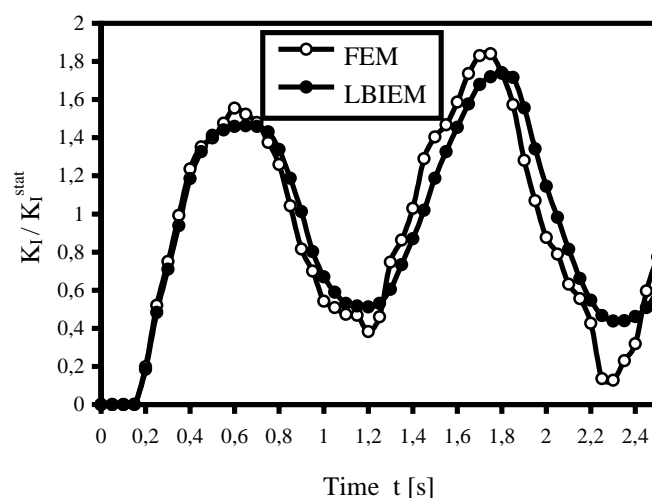


Fig. 4: Normalized dynamic stress intensity factor for a FGM plate with $E_2/E_1 = 0.2$

Acknowledgements: This work is supported by the Slovak Science and Technology Assistance Agency under APVT-51-003702, the Slovak Grant Agency under VEGA-2303823, and the Project for Bilateral Cooperation in Science and Technology supported jointly by the International Bureau of the German BMBF and the Ministry of Education of Slovak Republic under SVK 01/020.

REFERENCES

- [1] Sladek, J., Sladek, V. and Zhang, Ch. Application of meshless local Petrov-Galerkin (MLPG) method to elastodynamic problems in continuously nonhomogeneous solids. *Comp. Model. Eng. Sci.*, 4, 637-647 (2003).
- [2] Sladek, J., Sladek, V. and Van Keer, R. Meshless local boundary integral equation method for 2D elastodynamic problems. *Int. J. Num. Meth. Eng.*, 57, 235-249 (2003).
- [3] Atluri, S. N., Sladek, J., Sladek, V. and Zhu, T. The local boundary integral equation (LBIE) and its meshless implementation for linear elasticity. *Comput. Mech.*, 25, 180-198 (2000).
- [4] Belytschko, T., Krongauz, Y., Organ, D., Fleming, M. and Krysl, P. Meshless methods: An overview and recent developments. *Comp. Meth. Appl. Mech. Eng.*, 139, 3-47 (1996).
- [5] Stehfest, H. Algorithm 368: numerical inversion of Laplace transform. *Comm. Assoc. Comput. Math.*, 13, 47-49 (1970).
- [6] Kim, J. and Paulino, G. Finite element evaluation of mixed-mode stress intensity factors in functionally graded materials. *Int. J. Num. Meth. Eng.*, 53, 1903-1935 (2002).